HEAVY ION BEAM HEATED CYLINDERS: PLANNING FOR HOT DENSE MATTER EXPERIMENTS AT GSI

R. Arnold, J. Meyer-Ter-Vehn

JOURNAL DE PHYSIQUE
Colloque C8, supplément au n°11, Tome 44, novembre 1983

HEAVY ION BEAM HEATED CYLINDERS : PLANNING FOR HOT DENSE MATTER EXPERIMENTS AT GSI*

R. Arnold and J. Meyer-ter-Vehn

Max-Planck-Institut für Quantenoptik, D-8046 Garching, F.R.G.

Résumé

On présente des calculs de pouvoir d'arrêt pour des ions lourds de 1-100 GeV, et des simulations 1D et 2D de cibles cylindriques étirées, chauffées par d'intenses faisceaux d'ions lourds. Les projets d'expérience en cours de montage au GSI/Darmstadt et les domaines de physique à explorer sont discutés.

Abstract

Stopping power calculations for heavy ions of 1-100 GeV energy and results of 1D and 2D simulations of stretched target cylinders heated by intense heavy ion beams are presented. Plans to perform such experiments at GSI/Darmstadt and physics areas to be investigated are discussed.

1. Accelerator Opportunities for Heavy-Ion Target Physics at GSI

At GSI in Darmstadt there are firm plans to construct within the next few years a heavy-ion synchrotron (SIS) for fundamental nuclear research(1). The design parameters at present specify a ring with a rigidity of 18 Tesla-meters, and the machine is currently referred to as SIS-18. If an intense injector is added to this accelerator, e.g. using radio-frequency quadrupoles in the initial low-velocity section of the linac, it would be possible to fill the ring to its space-charge limit (at injection) of 10^{11}-10^{12} heavy ions of moderate charge-state. As a reference scenario, we consider I^{20+}. Acceleration to a final energy of 40 GeV would give a beam-pulse of a few hundred joules energy.

It is estimated that the emittance of such a beam would be sufficiently small to allow focussing on a spot of 100-150 μm radius(2). We estimate

*This work was supported by the Bundesministerium für Forschung und Technologie

that multiple scattering will cause no important increase in this spot size at the energies described here, for Au targets.

Using the calculated stopping power described later we find specific deposition energies with this beam of order 0.1-0.5 MJ/g are possible, depending upon the final fraction of the ion range which can be isolated and observed, and the specific assumptions on accelerator capacities.

To achieve specific power levels suitable for the targets we discuss, the beam pulse duration must be reduced by rebunching on a harmonic number of unity followed by longitudinal compression in the synchrotron ring before extraction. A fast extraction system must also be used. The feasibility of such modifications to SIS-18 has been studied(3) and it is estimated that pulse lengths as short as 20 ns can be achieved. The available beam power levels are thus of the order of 10^{-2} TW/mg and we have used this value as a guide in our theoretical survey of target responses.

2. Target Physics Considerations

2.1. Cylindrical Target Experiments: Introduction

We examine here the feasibility of a series of physics experiments including measurements of properties of hot, dense plasmas and their interactions with high energy heavy ion beams. Beams obtained from heavy-ion synchrotrons can have a low emittance, which allows a small focal spot radius and small beam divergence; but their high energy gives a range in matter much larger than the spot radius. Thus the heated plasma volume has the shape of a needle. This shape contrasts with disc or sphere target geometries used in other intense-beam technologies.

If the length in time of the beam pulse is short enough, the heated plasma volume will not cool by expansion faster than it is heated by the beam. The feasibility of experiments with needle targets was previously examined for protons(4). For solid, high-Z-targets with spot radii of 150 µm, the beam pulse should be no longer than 20 ns for optimum uniform heating of the plasma volume.

For the beam power levels available from the heavy-ion synchrotrons discussed here, a useful measure of target drive is the beam power deposited per unit mass of target. We will measure this specific power P in TW/mg, which is also MJ/g/NS.

Typical values of P considered here are .005 - .02 TW/mg. We have carried out numerical estimates of the temperatures and densities generated by a given specific power. For uniform targets and beams, the temperatures achievable in Au after 20 ns are shown in Figure 1. Areas of physics research accessible in plasmas of solid density of these temperatures are indicated on that figure; we discuss these areas individually below. Targets which utilize nonuniformities, and have important local hydrodynamic fluctuations, will be discussed later.

Scaling laws for uniform targets were discussed in reference 5, and these results are shown as solid lines in Figure 1.

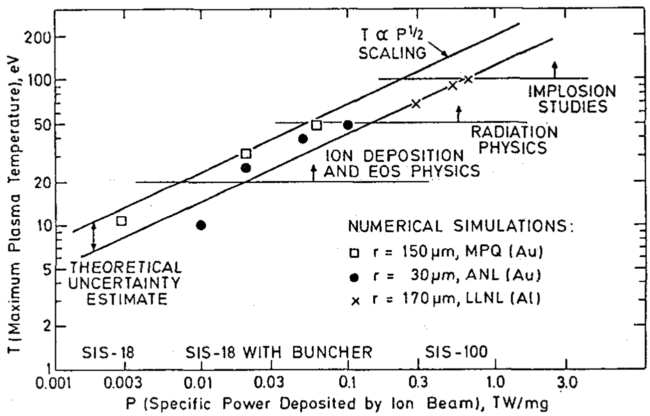

Figure 1: Plasma temperatures reached, in material directly heated by ion beam, 20 nanoseconds after beam is turned on at a constant power; uniform Au target, with one-dimensional calculations.

2.2. Ion-Beam Energy Deposition

Stopping powers and ranges of heavy ions in cold solid material have been measured at GSI up to energies of 10 MeV/nucleon for a number of projectile/target combinations(6). Extrapolations up to 100 MeV/nucleon have been tabulated by Hubert et al(7). Results of MPQ range calculations for some relevant projectile ions and solid gold as target are given in Fig. 2. In the lower energy regime they have been adjusted to the GSI data, for higher energies they have been calculated with standard stopping theory(8).

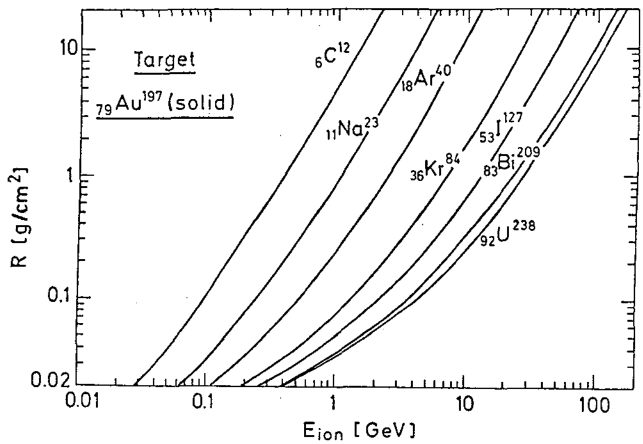

Figure 2: Calculated ranges for various ion beams in cold Au targets at solid density.

The stopping power is not constant along the stopping path, but has pronounced maximum at its end (Bragg peak). This peak is important for ions of moderate charge and a long range, as in our case here, although not in heavier ions at lower energies such as Bi at 10 GeV. In Fig. 3, the stopping power is plotted versus penetration depth for 40 GeV I ions in Au and for temperatures T = 0 eV and T = 100 eV. The range in hot material is shorter. Such predicted variations should be easily observable for plasma temperatures of 20 eV or greater.

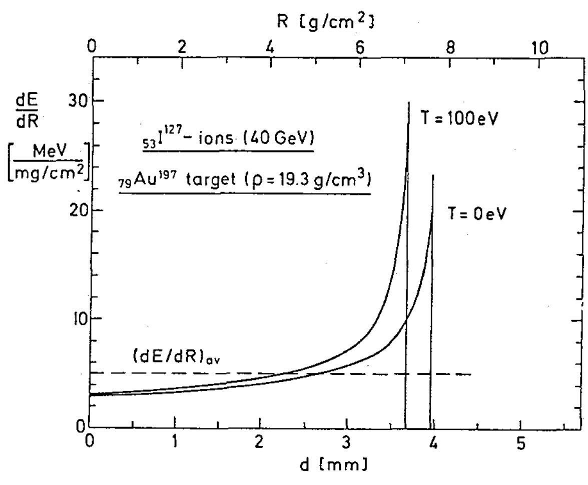

Figure 3: Calculated stopping power of iodine ions vs. penetration depth in Au targets, at solid density, for T = 0 and T = 100 eV.

2.3. Equation-of State Physics

Estimates for the pressure and internal energy of dense, hot plasmas are very important in predicting the performance of ICF targets. Theoretical models at present can provide an accurate equation of state (EOS) in three regions: dilute (ionized) gas, ultra-dense (highly degenerate) matter, and very-high-temperature (> 10 keV, fully ionized) nondegenerate plasma. However, many regions of interest (especially for ICF) remain without adequate theoretical understanding, including matter at compression factors of 10-1000 times and temperatures ranging up to 1 keV. This region includes in particular a largely unexplored region at low temperatures and high densities, where a variety of metallic phase transitions are predicted.

Prior EOS experiments at pressures greater than one Mbar have been carried out using strong shock waves induced by impact of projectiles from gas or rail-guns, intense pulses from lasers, charged particles from pulsed power diodes, imploding liners driven by explosively compressed magnetic fields, or by nuclear explosives. It is difficult (or impossible) in most of these experiments to achieve sufficiently isentropic compressions necessary to reach many interesting phase transition conditions. In addition, data collection rates are low, and reproducibility is often a problem.

Measurement of density responses in solid cylindrical targets heated centrally by high-energy ion beams provides a new technique for exploring EOS physics. The plasma uniformity, beam uniformity, and reproducibility should all be very good. With a pulse repetition rate of one per second possible, data acquisition rates would be limited by the time required to reposition new targets rather than by the driver, unless experimental techniques are developed to take advantage of such high rates.

Shell outward-compression factors of up to x8 (depending on EOS assumptions) are seen in our numerical simulation of expanding uniform cylinders, when the cylinder radius is much larger than the beam radius. The local density values reached are a sensitive measure of EOS. Inward compression of these rods, using hollow ion beams (with a central region blocked out, e.g. by an absorbing rod), can utilize cylindrical convergence to briefly reach factors of 30 - 50 times solid densities; pulse-shaping is necessary for this, as well as for isentropic-compression experiments.

2.4. Heat Transport

The hydrodynamic response of the target material depends not only on the beam deposition and EOS, but also on heat transport mechanisms. Thus, a study of target response will also reveal data on the basic mechanisms of heat flow in hot, dense plasmas. Three interesting transport mechanisms are expected to be excited in the dense targets we consider: electronic conduction, radiative transfer, and turbulent hydrodynamic convection.

As has been known for a long time, especially in astrophysical studies, the relative importance of these mechanisms varies widely, depending upon plasma temperature, density, and composition. Of the first two mechanisms, classical electronic heat conduction is thought to be the more significant for plasma densities of high Z near solid densities and at temperatures below 50 eV. However, in high-power laser target experiments, the electronic conduction is often found to be much less than the classical estimates of Spitzer. Experiments in dense, hot, ion-driven plasmas should be useful in understanding some of the determining factors for electronic conduction.

Radiative transport becomes the dominant mechanism for high temperatures in sufficiently dilute low-Z plasmas. The theoretical dependences of radiative transport coefficients (e.g. Rosseland mean opacity) on temperature, density, and composition is extremely complicated. Very little data is available, under controlled laboratory conditions, to compare against complex and uncertain theoretical calculations. When sufficiently hot regions in ion-driven targets with a sufficiently large plasma volumes can be generated, laboratory measurements should be possible.

2.5. Hydrodynamic Instabilities

Under the conditions of extreme pressures and temperatures expected in ICF targets, a wide variety of hydrodynamic instabilities are possible. An understanding of these is quite important for the development of ICF. Some mathematical modelling can be carried out with multidimensional numerical hydrodynamic computer codes, but many questions (especially nonlinear saturation of instabilities) will remain theoretically intractable. Experimental investigations cannot be scaled from conventional laboratory conditions, as in meteorology, because the material conditions are so extreme in ICF. Thus, controlled observation of instability development would be very valuable. Such experiments appear feasible with the cylindrical targets discussed here.

In uniform homogeneous cylindrical targets heated by high-energy ion beams the outward expansion is driven by a low-density, high-pressure interior core, which pushes outward, compressing and accelerating the (denser) surrounding shell. As in the spherical implosion case, this is a condition for developing Rayleigh-Taylor instability, leading to disruption of the cylindrical symmetry. For perturbation wavelengths short compared to the cylinder radius (~ 100 µm) and for times short compared to the cylinder expansion time ($\sim 10^{-7}$ sec.), the nonlinear dynamics is the same as in plane geometry, or in spherical geometry at early times in an implosion history.

Thus, data can be gathered directly in a region of interest to ICF target design, if the R-T instability development is studied in the targets described here.

Another hydrodynamic nonlinear phenomenon which can be expected is the Benard (convective) instability. When a layer of fluid is accelerated, with a thermal gradient opposite to the acceleration direction, convection will begin. As the ratio of bouyant forces to acceleration (Rayleigh number) increases, the internal fluid motion will become turbulent; heat transport will increase with temperature faster than without convective-turbulent behaviour. In ICF targets, this will not necessarily lead to disruption, but it can have a profound effect on the heat flow and implosion dynamics. Such hydrodynamic phenomena can be studied, at plasma conditions similar to those encountered in the early implosion history of ICF targets, in some cylindrical ion-driven target configurations.

3. Hydrodynamic Simulations of Plasma Cylinders

3.1. One-Dimensional Calculations

To estimate the hydrodynamic phenomena induced in the target volumes, the effects of these on target heating, and provide a first look at possible experimental measurements of EOS, etc., a series of numerical calculations has been carried out. One-dimensional calculations (radial) have been carried out using a hydrodynamic code at MPQ named LAPLAS. It has been adjusted to simulate the cylindrical-target, high-energy ion-beam experiments described here, and to include a realistic EOS.

Electronic heat conduction is included, estimated by the classical Spitzer formulas. This may be an overestimate, but even so, heat conduction plays only a small role in our calculations. Radiative transfer is not presently included, but this should not be important for temperatures below 50 eV in the targets we simulate.

The beam is turned on at t = 0 and continues at a constant power level, and the response of the target material is calculated as function of space and time. After a time of order 20 ns the temperature reaches a plateau, as the expansion of the heated plasma volume cools the core as fast as the beam heats it.

A typical case with beam power .015 TW/mg. is shown in figures 4 and 5, which show density and temperature profiles. The temperature plateau, around 20 ns, is clearly evident.

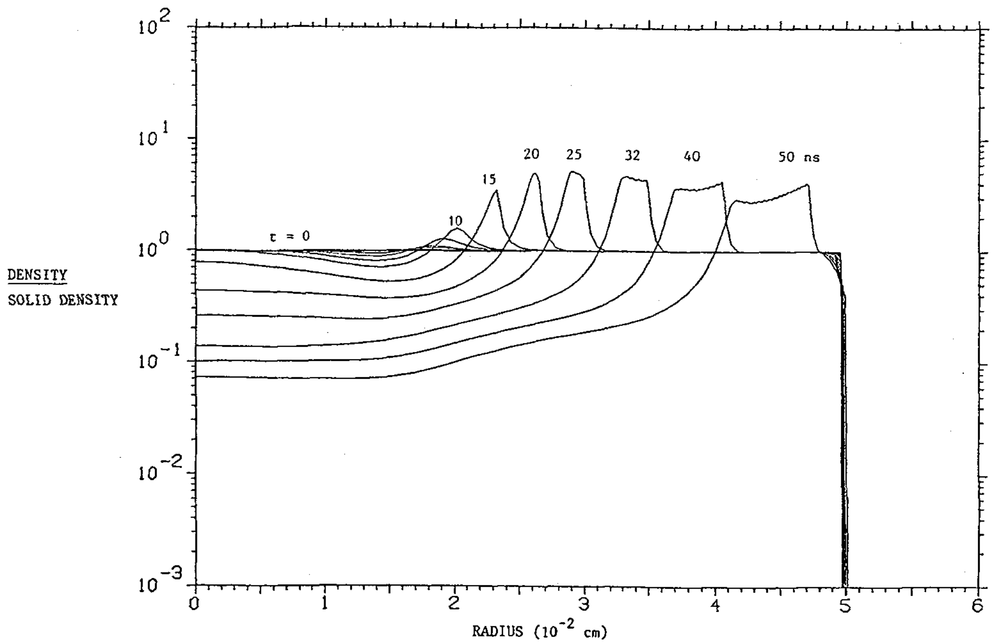

Figure 4: Density profiles in a solid, homogeneous Au rod, with outer radius 500 µm, axially heated by an ion beam with specific deposition power of .015 TW/mg

A series of such simulations extended to higher powers was also carried out. It is found, especially at the powers exceeding .015 TW/mg., that pulse lengths up to 50 ns may be useful, which take the target temperatures to considerably higher values than given in Figure 1. The temperature is, however, limited by the specific energy available from the beam (time-integral of the specific power) in the accelerator scenarios discussed here.

Numerical simulations have also been carried out for targets which have a core volume of reduced density compared to the outer shell. If the beam directly heats only the underdense core, we find that a longer time is available for heat accumulation compared to uniform targets, and thus higher temperatures (but lower pressures) can be reached, provided the beam power can be maintained for a sufficiently long time. At P = .015 TW/mg, temperatures higher than the plateau value seen in homogeneous targets by a factor of 2 can be reached at 30 ns.

The temperature in a small region near the axis can be greatly increased for a short time by utilizing a target with an underdense core, with the beam heating directly the dense shell. This arrangement allows the core to collapse and compress the thin material at the center to high temperatures, e.g. 100 eV, even with relatively low driving power (P ~ .005 TW/mg). This method could be used to extend stopping-power measurements to high temperatures even at low beam powers.

3.2. Two Dimensional Calculations

One-dimensional simulation gives a first picture of how ion heated cylinders behave. Some important aspects, however, become clear only in two-dimensional calculations. As an example, a case is shown in Fig. 6, in which a homogeneous 2 mm Al foil is heated by a uniform, continuous beam with sharp edge at 200 µm radius and uniform deposition power of P = 0.004 TW/mg. The beam is stopped initially at half the foil thickness.

The results, shown in Fig. 6 as cuts through the heated cylinders at different times, have been obtained with a 2D PIC-Code, developed at MPQ by P. Mulser and D. Lackner-Russo[9]. The point densities correspond to the matter densities. At time t = 18 ns, one clearly recognizes the heated cylinder. A cylindrical shock wave is running outwards from its surface and a rarefaction wave inwards. Corresponding waves are seen at

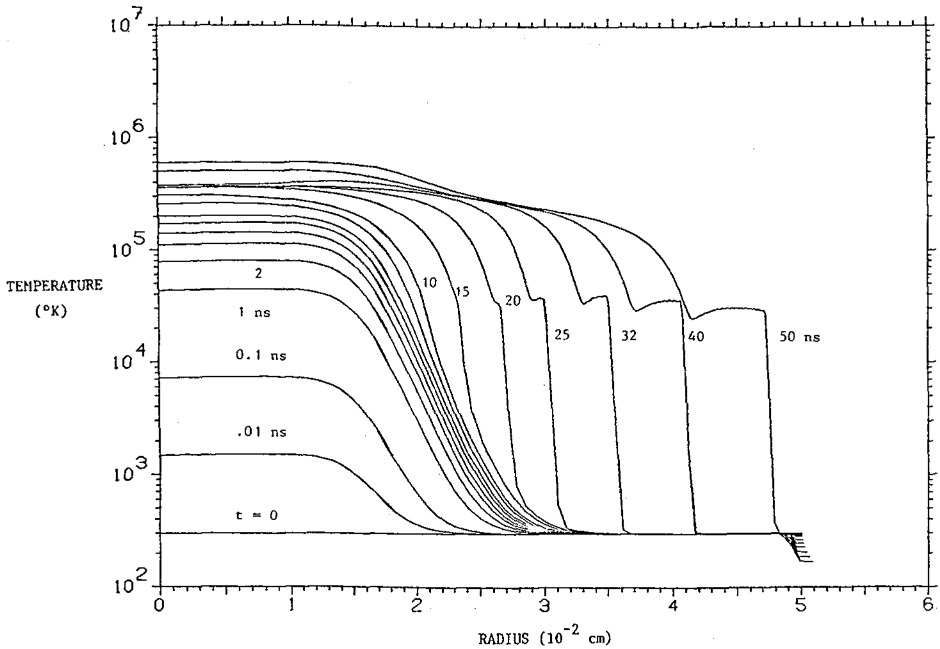

Figure 5: Temperature profiles of a uniform target, as in Figure 4.

the front sides. At t = 34 ns, the originally heated volume has been rarified almost completely, and target material is streaming out at the front side. The ion beam can now penetrate more deeply. The deeper penetration starts at the outer regions of the heated cylinder since here rarefaction sets in first. Thus it is a type of hollow beam which reaches the inner target regions first where now shock waves are running inwards as well as outwards. This is clearly seen in Fig. 6 at t = 34 ns. The imploding compression wave finally produces a region of high density matter on the cylinder axis as seen at t = 58 ns. At this time, the beam has burned a hole through the 2 mm foil.

It is seen that the ion beam can penetrate into the target beyond its initial stopping length. These and other interesting hydrodynamic phenomena can be investigated already with beams of moderate intensity.

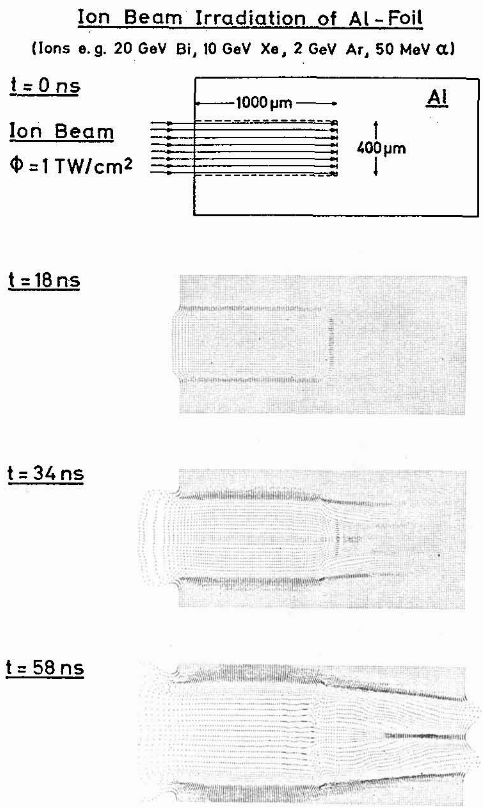

Figure 6: Two-dimensional simulation of the penetration of an ion beam into an Alumium foil 2 mm thick.

References

1.) GSI design report, SIS (1981).

2.) I. Hoffmann and H. Wollnick (private communication).

3.) R. Müller (private communication).

4. R.C. Arnold et al., Nucl. Instr. and Methods 199, 557 (1982).

5.) J. Meyer-ter-Vehn, Proc. Symp. Acc. Aspects of Heavy Ion Fusion, Report GSI-82-8, 1982, p. 514.

6.) H. Geissel et al., ibid., p. 578.

7.) F. Hubert et al., Suppl. Ann. de Physique 5, 1 (1980).

8.) J. Meyer-ter-Vehn, N. Metzler, "Target Design for Heavy Ion Fusion", Report MPQ 48, 1981, MPI Quantum Optics, Garching/FRG.

9.) D. Lackner-Russo, P. Mulser, "A Macroscopic PIC Code for Beam Target Interaction Studies", Report PLF 32 (1980), MPI Quantenoptik, Garching.